

# Intercalation route to nano-hybrids: inorganic/organic-high $T_c$ cuprate hybrid materials†

Jin-Ho Choy, Soon-Jae Kwon, Seong-Ju Hwang, Young-Il Kim and Woo Lee

Department of Chemistry, Center for Molecular Catalysis, College of Natural Sciences, Seoul National University, Seoul 151-742, Korea. E-mail: jhchoy@plaza.snu.ac.kr

Received 20th April 1998, Accepted 27th July 1998

A systematic application of intercalation techniques to layered superconducting oxides enables us to open a new chapter in the development of nano-hybrids with various functions. Recently we were successful in preparing a new series of inorganic–inorganic nano-hybrids,  $M-X-Bi_2Sr_2Ca_{m-1}Cu_mO_y$  ( $M = Hg, Ag, Au$ ;  $X = Br, I$ ;  $m = 1-3$ ) and organic–inorganic ones,  $R_2HgI_4-Bi_2Sr_2Ca_{m-1}Cu_mO_y$  ( $R =$  organic cation). Our synthetic strategies are based on (1) HSAB (hard–soft acid–base) interactions and (2) interlayer complexation concepts. Since the iodine species in  $IBi_2Sr_2Ca_{m-1}Cu_mO_y$  are stabilized as  $I_3^-$  (soft base) with a charge transfer between host and guest, soft Lewis acids like  $Ag^+$ ,  $Au^+$ , and  $Hg^{2+}$  can be further intercalated into the iodine layers inbetween the (Bi–O) double layers. On the other hand, new organic–inorganic nano-hybrids ( $R_2HgI_4-Bi_2Sr_2Ca_{m-1}Cu_mO_y$ ) have also been achieved through the intercalative complex-salt formation reaction between preintercalated  $HgI_2$  molecules and  $R^+I^-$  salts in the interlayer space of  $Bi_2Sr_2Ca_{m-1}Cu_mO_y$ . Compared to the pure compounds the superconducting transition temperatures of the organic-salt intercalates are little changed even with a large basal increment upon intercalation, indicating a two-dimensional nature of the high- $T_c$  superconductivity. From the viewpoint of application, the intercalation of large organic molecules provides a new synthetic route to high- $T_c$  superconducting thin-film and nano-particles by separating superconducting blocks into isolated single sheets.

## Introduction

Intercalation techniques have been widely applied not only to the study of chemical and physical properties of low dimensional compounds but also to the development of new nano-hybrid materials that cannot be prepared by conventional solid state methods.<sup>1</sup> The essential advantage of this technique is that it allows some degree of modification in the geometric, chemical, electronic, and optical properties of host and guest. Moreover, the bonding between them also varies broadly from essentially van der Waals dipolar to metallic and ionic. In this respect, intercalation reactions can be considered as effective tools in tailoring the properties of the desired materials and also in the investigation of the physical properties of layered materials.

Since the discovery of high- $T_c$  superconductivity in ceramic cuprate materials, intense research efforts have been made to understand their high- $T_c$  superconductivity, but the mechanism has not yet been established. Concerning the high- $T_c$  superconducting mechanism, one of the most important debating points is on the relationship between the superconductivity and structural anisotropy which is a common feature of high- $T_c$  superconductors. Actually it is expected that the superconductivity can be affected by the interlayer Josephson coupling which depends on the interlayer distance of the  $CuO_2$  layer. On the other hand, instead of Josephson coupling, Wheatley, Hsu, and Anderson considered the coherent hopping of valence bond pairs between  $CuO_2$  planes (WHA model).<sup>2</sup> However, the validity of these theoretical models has remained unconfirmed due to the lack of experimental evidence. If we can control the strength of interlayer coupling, it will be informative in understanding the relation between interlayer coupling and superconductivity. In this regard, the intercalation into high- $T_c$  superconductors is expected to be quite effective because it allows us to control the strength of inter-

layer coupling. Further, intercalation can also provide useful ways of preparing high- $T_c$  superconducting nano-hybrids with multi-functional properties since it enables us to combine the heterogeneous species into a unified chemical system.<sup>3-10</sup> From the viewpoint of practical application, it can also be expected that the high- $T_c$  superconducting intercalate with a remarkable lattice expansion will be available as a precursor for making superconducting thin-films and nano-particles, because the bulky guest molecule can facilitate the exfoliation of superconducting layers by minimizing the chemical interaction between superconducting blocks.<sup>7</sup>

As mentioned above the advantages of the intercalation technique have attracted us to perform systematic studies on high- $T_c$  superconducting intercalation compounds. Previously we have investigated the bonding character of iodine intercalated in  $Bi_2Sr_2Ca_{m-1}Cu_mO_y$  (denoted hereafter as Bi2201 for  $m=1$ , Bi2212 for  $m=2$ , and Bi2223 for  $m=3$ , respectively), and found that there is a partial electron transfer from host lattice to intercalant layer.<sup>10</sup> On the basis of such a finding, we can successfully develop a new series of inorganic–inorganic and organic–inorganic superconducting nano-hybrids by applying new synthetic strategies such as soft–hard acid–base interactions and the interlayer complexation concept.

In this paper, we report a systematic approach towards the synthesis of  $HgX_{2-}$ ,  $AgI^-$ , and organic-salt-intercalated  $Bi_2Sr_2Ca_{m-1}Cu_mO_y$  ( $m=1-3$ ), together with the characterization of their physico-chemical properties. Emphasis is especially placed on the synthetic strategies applied to develop the present inorganic–inorganic and organic–inorganic nano-hybrids.

## Experimental

All the pure  $Bi_2Sr_2Ca_{m-1}Cu_mO_y$  ( $m=1-3$ ) compounds were prepared by the conventional solid state reaction. At first, the powder reagents  $Bi_2O_3$ ,  $PbO$ ,  $SrCO_3$ ,  $La_2O_3$ ,  $CaCO_3$ , and  $CuO$  were thoroughly mixed with molar ratios of Bi: Sr: La: Cu = 2: 1.6: 0.4: 1 for  $m=1$ , Bi: Sr: Ca: Cu = 2: 1.5: 1.5: 2 for  $m=2$ , and Bi: Pb: Sr: Ca: Cu = 1.85: 0.35: 1.9: 2.1: 3.1 for  $m=3$ ,

†Basis of the presentation given at Materials Chemistry Discussion No. 1, 24–26 September 1998, ICMCB, University of Bordeaux, France.

respectively and the obtained mixtures were calcined at 800 °C for 12 h in air, and then, the pre-fired materials were pressed into 13 mm disc-shaped pellets and finally sintered with intermittent grinding. Depending upon the composition, different final heating conditions were adopted to obtain the single phase samples. That is, the pure  $\text{Bi}_2\text{Sr}_2\text{CuO}_y$  (Bi2201) and  $\text{Bi}_2\text{Sr}_2\text{CaCu}_2\text{O}_y$  (Bi2212) compounds were prepared by heating for 40 hours in air at 890 and 860 °C, respectively, whilst the pure  $\text{Bi}_2\text{Sr}_2\text{Ca}_2\text{Cu}_3\text{O}_y$  (Bi2223) sample was synthesized by heating at 830 °C for 150 h in a  $\text{N}_2$  (99.999%) atmosphere. Since the stoichiometric  $\text{Bi}_2\text{Sr}_2\text{CuO}_y$  compound possesses an overdoped hole concentration, some of the  $\text{Sr}^{\text{II}}$  ions (20%) were substituted with  $\text{La}^{\text{III}}$  to induce the highest  $T_c$  with an optimum hole concentration.<sup>11</sup> In the case of the Bi2223 phase, both the substitution of  $\text{Bi}^{\text{III}}$  ion with  $\text{Pb}^{\text{II}}$  and heat treatment in a reduced atmosphere were required to obtain a single phase sample,<sup>12</sup> since such conditions make it easier to form Bi2223 through the reaction between the intermediate products Bi2212 and  $\text{Ca-Sr-Cu-O}$ .<sup>13</sup> The  $\text{HgX}_2$ -intercalates ( $\text{X} = \text{Br}$  or  $\text{I}$ ) were synthesized by vapor transport reaction between host and guest in a vacuum sealed Pyrex tube. In the case of Bi2201 and Bi2212, their  $\text{HgBr}_2$ -intercalates were easily obtained by heating the pure compounds with excess  $\text{HgBr}_2$  at 230 °C for 4 h, while their  $\text{HgI}_2$ -intercalates were prepared by heating the pure samples with excess  $\text{HgI}_2$  at 190 °C for 2 h and then at 240 °C for 4 h with one molar equivalent of free iodine as a transport agent.<sup>4</sup> However, the intercalation of  $\text{HgX}_2$  into Bi2223 could not be achieved through the direct reaction between host and  $\text{HgX}_2$  vapor. In order to overcome such a difficulty, we have used iodine intercalated Bi2223 as a secondary host, which results in the formation of the first-stage intercalate. On the other hand, each AgI-intercalate of Bi2201 and Bi2212 was synthesized by heating a mixture, in the form of a pellet, of the pure compound and Ag metal under an iodine atmosphere [ $P(\text{I}_2) = 1$  atm]. The heat treatment was carried out in a stepwise manner where the sample was heated in an iodine atmosphere at 170 °C for 3 h and then in air at 190 °C for 10 h. According to the X-ray diffraction (XRD) analysis for the product after the first heat treatment at 170 °C, it was found that no AgI-intercalate exists but the iodine-intercalate is formed together with AgI. Such a finding indicates that the AgI intercalation is accomplished *via* the thermal diffusion of  $\text{Ag}^+$  ions into the preintercalated iodine sublattice.<sup>14</sup> However, the AgI-intercalated Bi2223 was not easily prepared by the above method as in the case of  $\text{HgX}_2$ -Bi2223, which is attributed to the high deintercalation rate of preintercalated iodine compared to the  $\text{Ag}^+$  diffusion rate into the lattice. For this reason, we have adopted an alternative synthetic route whereby a mixture of AgI and iodine-intercalated Bi2223 (IBi2223) was heated at 190 °C for 75 h under an iodine vapor pressure of 1 atm. The single phase AgI-intercalate could be finally obtained by both extending the reaction time and imposing an iodine atmosphere to prevent iodine disintercalation during  $\text{Ag}^+$  diffusion. Such a difficulty in the intercalation of  $\text{HgX}_2$  and AgI into Bi2223 is attributed to the fact that the pure sample cannot suffer from a large elastic deformation upon intercalation owing to its thicker unit block with three  $\text{CuO}_2$  layers compared to Bi2201 and Bi2212. This is also partially ascribed to an enhanced attraction between  $\text{BiO}$  layers induced by the substitution of  $\text{Bi}^{\text{III}}$  with  $\text{Pb}^{\text{II}}$ .<sup>15</sup>

The organic-inorganic hybrids  $[(\text{Py-C}_n\text{H}_{2n+1}\text{I})_2\text{HgI}_4] \cdot \text{Bi}_2\text{Sr}_2\text{Ca}_{m-1}\text{Cu}_m\text{O}_y$  ( $n = 1, 2, 4, 6, 8, 10, \text{ or } 12$ ;  $m = 1-3$ ) were synthesized by the stepwise intercalation route as follows; first, the  $\text{HgI}_2$ -intercalates were prepared as mentioned above, and then, the intercalation of the organic chain was carried out by the solvent-mediated reaction between the  $\text{HgI}_2$ -intercalate and alkylpyridinium iodide. The reactants  $\text{Py-C}_n\text{H}_{2n+1}\text{I}$  ( $n = 1, 2, 4, 6, 8, 10, \text{ or } 12$ ) were prepared by the reaction between equimolar amounts of alkyl iodide and pyridine in diethyl ether. The  $\text{HgI}_2$ -intercalates were mixed with two molar excess

of  $\text{Py-C}_n\text{H}_{2n+1}\text{I}$ , to which a small amount of pure acetone was added. Each mixture was reacted in a closed ampoule at 40–70 °C for 6 h and washed with a mixture of acetone and diethyl ether in order to remove the excess  $\text{Py-C}_n\text{H}_{2n+1}\text{I}$ . The resulting products were dried under vacuum. All the samples were air-stable, which made the characterization of their physico-chemical properties easier.

The physico-chemical characterizations were carried out with X-ray diffraction (XRD) and dc magnetic susceptibility measurements along with chemical analysis by electron probe micro-analysis (EPMA) and thermogravimetric analysis (TGA). In the case of the AgI-intercalates, their ionic conductivity was measured in the temperature range 25–270 °C with impedance spectroscopy. The electronic configuration and the crystal structure of the intercalation compounds were investigated by performing X-ray absorption spectroscopic (XAS) analyses, which were carried out on the beam lines 7C and 10B at the Photon Factory, National Laboratory for High Energy Physics (KEK-PF) in Tsukuba. The applied synchrotron X-ray radiation was provided by a storage ring of a 2.5 GeV electron beam with a current of *ca.* 300–360 mA.

## Results and discussion

### Iodine intercalation

It is well known that intercalation reactions occur in highly anisotropic lamella structures in which the interlayer binding forces are fairly weak compared to the strong ionocovalent intralayer ones. In this respect, the weak van der Waals interaction between the  $\text{Bi}_2\text{O}_2$  layers in layered Bi-based cuprate superconductors allows these compounds to be good host materials for intercalation reaction as shown in Fig. 1.<sup>16</sup>

As we were performing our research in this field, some organic and inorganic molecules were reported in the literature to be intercalated into the Bi-based cuprate high- $T_c$  superconductors (Table 1). However, among them, only the iodine intercalation compound has been chemically well defined. From the magnetic susceptibility and four probe resistivity measurements for the iodine intercalates, we found that the  $T_c$  is depressed by  $\approx 10$  K upon iodine intercalation.<sup>10</sup> Since the  $T_c$  of cuprate superconductors is closely related to the hole concentration in the  $\text{CuO}_2$  plane, we have examined the bonding character of iodine stabilized in the lattice of IBi2212 with Raman and X-ray absorption near edge structure

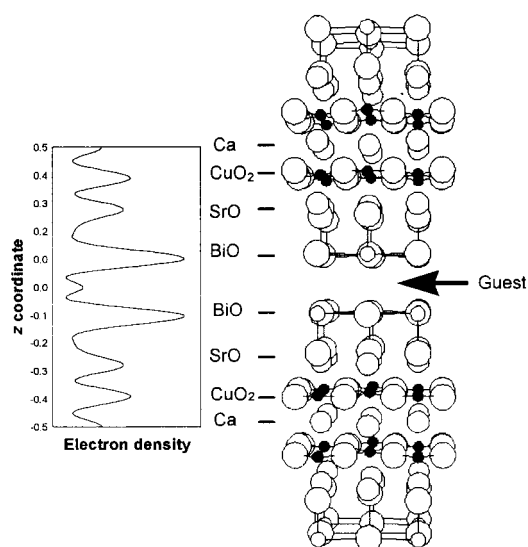


**Fig. 1** Mica-like crystal structure of the Bi2212 superconductor, together with a one-dimensional electron density map along the  $c$ -axis. The guest species can be intercalated inbetween weakly bound  $\text{Bi}_2\text{O}_2$  double layers.

**Table 1** High- $T_c$  superconducting intercalation compounds

Intercalant	Research group	Published in	Year
Iodine <sup>a</sup>	X. D. Xiang <i>et al.</i>	<i>Nature</i> , <b>348</b> , 145	1990
Copper, silver	G. A. Scholz <i>et al.</i>	<i>Solid State Commun.</i> , <b>74</b> , 959	1990
Lithium	T. Okubo <i>et al.</i>	<i>Physica C</i> , <b>185–189</b> , 847	1991
Bromine	Y. Koike <i>et al.</i>	<i>Solid State Commun.</i> , <b>79</b> , 501	1991
IBr	M. Mochida <i>et al.</i>	<i>Physica C</i> , <b>212</b> , 191	1993
Conjugated ring organic molecules	L. S. Grigorian <i>et al.</i>	<i>Physica C</i> , <b>205</b> , 296	1993
Metal-phthalocyanines	L.S. Grigorian <i>et al.</i>	<i>Physica C</i> , <b>218</b> , 153	1993
Hg <sub>2</sub> Cl <sub>2</sub>	Y. Muraoka <i>et al.</i>	<i>Physica C</i> , <b>233</b> , 247	1994
Fullerene (C <sub>60</sub> )	S. Sathaiah <i>et al.</i>	<i>J. Appl. Phys.</i> , <b>81</b> , 2400	1997

<sup>a</sup>Only the iodine intercalate is chemically well-defined.

**Table 2** Previous reports on the iodine intercalated Bi-cuprates, those which are classified, depending upon the author's interpretation of why the  $T_c$  is depressed upon iodine intercalation

Charge transfer	Interlayer coupling
J. H. Choy <i>et al.</i> , <i>J. Solid State Chem.</i> , <b>102</b> , 284 (1993)	X. D. Xiang <i>et al.</i> <i>Nature</i> , <b>348</b> , 145 (1990)
D. Pooke <i>et al.</i> <i>Physica C</i> , <b>198</b> , 349 (1992)	X. D. Xiang <i>et al.</i> <i>Science</i> , <b>254</b> , 1487 (1991)
T. Huang <i>et al.</i> <i>Phys. Rev. B</i> , <b>49</b> , 9885 (1994)	P. V. Huong <i>et al.</i> <i>Phys. Rev. B</i> , <b>48</b> , 9869 (1993)
Y. Koike <i>et al.</i> <i>Physica C</i> , <b>208</b> , 363 (1993)	J. Ma <i>et al.</i> <i>Physica C</i> , <b>227</b> , 371 (1994)
M. A. Subramanian, <i>J. Solid State Chem.</i> , <b>110</b> , 193 (1994)	M. Biagini, <i>Phys. Rev. B</i> , <b>52</b> , 7715 (1995)
C. K. Subramaniam <i>et al.</i> <i>Physica C</i> , <b>249</b> , 139 (1995)	

(XANES) spectroscopies. The Raman spectroscopic results indicated that the intercalated iodine is stabilized as a triiodide molecular ion ( $I_3^-$ ),<sup>17</sup> which was also confirmed by the I L<sub>1</sub>-edge XANES analysis.<sup>10</sup> Further evidence on the hole donation from the intercalated iodine layer to the superconducting CuO<sub>2</sub> layer could be obtained from the thermoelectric power and the Cu K-edge XANES analyses.<sup>18</sup> From these experimental findings, it was suggested that the  $T_c$  evolution upon iodine intercalation is due to the hole over doping to the CuO<sub>2</sub> sheets (Table 2).<sup>10,19</sup> However, on the basis of WHA model, other groups explained the  $T_c$  decrease for the first- and second-stage iodine intercalated compounds by the weakening of the interblock coupling due to the lattice expansion.<sup>2,20</sup> In fact, since it is impossible to separate both effects of intercalation, that is, lattice expansion effects and charge transfer ones, for the iodine intercalate, the origin of the  $T_c$  variation upon intercalation has remained controversial, as demonstrated in Table 2. In order to solve this problem, a new intercalation system, where the lattice expansion is larger than that of iodine intercalate, was required.

### Metal halide intercalation

From the Raman and XANES studies on the iodine intercalate, it becomes clear that the guest iodine plays a role as electron acceptor, that is, soft Lewis acid, with the host Bi-based superconductor as electron donor, soft Lewis base. It is therefore concluded that the driving force of iodine intercalation into Bi-based cuprates is a charge transfer between host and guest, and that an electronegative element or molecule can be incorporated into this superconducting lattice. Based on this understanding, we have tried to intercalate various kinds of soft (hard) Lewis acids which are classified in Table 3.<sup>21</sup> And as a result, we were successful in developing a new type of high- $T_c$  superconducting compound, M-X-Bi<sub>2</sub>Sr<sub>2</sub>Ca<sub>m-1</sub>Cu<sub>m</sub>O<sub>y</sub> (M=Hg, Ag, Au; X=Br, I; m=1–3), where a superconducting layer and an insulating/superionic conducting one are regularly interstratified.

According to the XRD (Cu-K $\alpha$  radiation) analyses, the lattice expansion along the  $c$ -axis ( $\Delta d$ ) upon intercalation is estimated to be  $\approx 6.3$  Å for HgBr<sub>2</sub>-intercalates and  $\approx 7.2$  Å for HgI<sub>2</sub> ones, which indicates that the halogen bilayers are stabilized in the interlayer space of Bi-based cuprates. According to the dc magnetic susceptibility measurements, all the metal halide-intercalates are found to exhibit bulk super-

**Table 3** List of Lewis soft acid–base compounds (ref. 18)

Lewis acid	Lewis base
Co(CN) <sub>5</sub> <sup>3-</sup> , Pd <sup>2+</sup> , Pt <sup>2+</sup> , Cu <sup>+</sup> , Ag <sup>+</sup> , Au <sup>+</sup> , Cd <sup>2+</sup> , Hg <sub>2</sub> <sup>2+</sup> , Hg <sup>2+</sup> , CH <sub>3</sub> Hg <sup>+</sup> , BH <sub>3</sub> , Ga(CH <sub>3</sub> ) <sub>3</sub> , GaCl <sub>3</sub> , GaBr <sub>3</sub> , GaI <sub>3</sub> , Tl <sup>+</sup> , Tl(CH <sub>3</sub> ) <sub>3</sub> , CH <sub>2</sub> , carbenes, HO <sup>+</sup> , RO <sup>+</sup> , RS <sup>+</sup> , RSe <sup>+</sup> , Te <sup>4+</sup> , RTe <sup>+</sup> , Br <sub>2</sub> , Br <sup>+</sup> , I <sub>2</sub> , I <sup>+</sup> , ICN, O, Cl, Br, I, N, M <sup>0</sup> (metal atoms), $\pi$ -acceptors; trinitrobenzene, quinones, <i>etc.</i>	H <sup>-</sup> , R <sup>-</sup> , C <sub>2</sub> H <sub>4</sub> , C <sub>5</sub> H <sub>6</sub> , CN <sup>-</sup> , RNC, CO, SCN <sup>-</sup> , R <sub>3</sub> P, (RO) <sub>3</sub> P, R <sub>3</sub> As, R <sub>2</sub> S, RSH, RS <sup>-</sup> , S <sub>2</sub> O <sub>3</sub> <sup>2-</sup> , I <sup>-</sup> , I <sub>3</sub> <sup>-</sup>

<sup>a</sup>All the elements intercalated into Bi<sub>2</sub>Sr<sub>2</sub>Ca<sub>m-1</sub>Cu<sub>m</sub>O<sub>y</sub> belong to the soft Lewis acid group and are denoted as *italic* characters.

conductivity with a slight  $T_c$  depression of only 6–14% compared to the corresponding pure materials. Their superconducting transition temperatures ( $T_c$ 's) are summarized in Table 4, together with lattice parameters. It was previously suggested that the  $T_c$  evolution upon intercalation might be due to a change in hole concentration in the CuO<sub>2</sub> planes<sup>10,19</sup> and/or due to the weakening of interblock electronic coupling.<sup>2,20</sup> Taking into account the hybrid structure of these intercalates where the electronically insulating metal halide layer is regularly interstratified between the superconducting lattices, the interblock electronic coupling is expected to be

**Table 4** Lattice parameters and superconducting transition temperatures of Bi<sub>2</sub>Sr<sub>2</sub>Ca<sub>m-1</sub>Cu<sub>m</sub>O<sub>y</sub> and their metal halide-intercalates

Compound	Metal halide	$a/\text{Å}$	$c/\text{Å}$	$\Delta d/\text{Å}$	$T_c/\text{K}$	$\Delta T_c/\text{K}$	
$m=1$	Pure	5.39	24.2		29		
	Intercalate	HgBr <sub>2</sub>	5.40	36.8	6.3	27	-2
		HgI <sub>2</sub>	5.39	38.4	7.1	25	-4
$m=2$	Pure	5.40	30.70		78		
	Intercalate	HgBr <sub>2</sub>	5.39	43.3	6.1	71	-7
		HgI <sub>2</sub>	5.40	45.0	7.2	68	-10
$m=3$	Pristine	5.40	40.0		105		
	Intercalate	HgI <sub>2</sub>	5.42	51.0	7.0	97	-8

$a$ : in-plane lattice parameter,  $c$ : out-of-plane lattice parameter,  $\Delta d$ : lattice expansion along  $c$ -axis per each metal halide layer,  $\Delta T_c = T_c$  (intercalate) -  $T_c$  (pure).

extremely weak. In this respect, the maintenance of superconductivity upon intercalation of metal halides allows us to conclude that interlayer coupling is not a main factor for superconductivity. It is also suggested that the present  $T_c$  evolution upon intercalation should be understood in terms of the charge transfer between guest and host block.

In this regard, we have performed XANES analysis for these intercalates in order to investigate the evolution of electronic configuration of host and guest upon intercalation. A comparison of the I  $L_1$ -edge XANES spectra for  $\text{HgI}_2$ -intercalates with that for the unintercalated  $\text{HgI}_2$  as a reference indicates clearly that there is a partial electron transfer from host block to guest  $\text{HgI}_2$  layer. The Br K-edge XANES analysis for  $\text{HgBr}_2$ -intercalate also reveals a partial electron transfer from host lattice to  $\text{HgBr}_2$  layer. From these XANES results, it becomes obvious that there is also a charge transfer between host and guest for all the metal halide intercalates, related to the  $T_c$  evolution upon intercalation, and that the intercalation of metal halide is surely a kind of Lewis acid-base reaction.

The intracrystalline structures of intercalated metal halide layers have also been investigated by performing extended X-ray absorption fine structure (EXAFS) analysis. In the case of  $\text{AgI}$ -intercalates, the experimental Ag K-edge EXAFS spectra are well fitted to the calculated data from a two-shell model where there is a displacement of Ag toward a face of the iodine tetrahedron, which is strikingly similar to the local structure of super-ionic conducting  $\alpha\text{-AgI}$ .<sup>22</sup> On the basis of this structural information, we have carried out ionic conductivity measurements for  $\text{AgI}$ -intercalates, and found that these compounds have a high ionic conductivity ( $\sigma_i = 10^{-1.4} - 10^{-2.6} \Omega^{-1}\text{cm}^{-1}$  at 270 °C) with uniform activation energies ( $\Delta E_a = 0.22 \pm 0.02$  eV), which are similar to those of other two-dimensional  $\text{Ag}^+$  superionic conductors.<sup>23,24</sup> Such ionic conductivity enables us to intercalate electrochemically the  $\text{Ag}^+$  ion into the lattice of  $\text{IBi2212}$  with the electrochemical cell  $-\text{Ag}|\text{AgI}_6\text{WO}_4|\text{IBi2212}-$ , where the contact between electrolyte and electrodes was improved through heat treatment. The ionic conduction in these compounds may attract special interest since the materials exhibit both high electronic and ionic conductivities with ionic transfer numbers of  $t_i = 0.02 - 0.60$ . Although it is rarely observed that a material possesses both high electronic conductivity and a high ionic one, the mixed conductivity of the  $\text{AgI}$  derivatives originates from their unique crystal structures consisting of an ionic conducting  $\text{AgI}$  layer and an electronic conducting host.

On the other hand, the Hg  $L_{III}$ -edge EXAFS fitting results indicate that the intercalated mercuric halide is stabilized as a linear molecule with bond distances of  $\approx 2.46$  Å for  $\text{HgBr}_2$ -intercalates and  $\approx 2.65$  Å for  $\text{HgI}_2$  ones, respectively. These intracrystalline structures of intercalated mercuric halides are quite similar to the local structures of free  $\text{HgX}_2$  vapors.<sup>25</sup> In this respect, the present EXAFS results clarify that these  $\text{HgX}_2$ -intercalates are the first examples of two-coordinated mercuric halide molecular solids stabilized in an ionocovalent solid matrix. As shown in Fig. 2, we suggest a structural model for mercuric halide intercalates, based on the present Hg  $L_{III}$ -edge EXAFS results and one-dimensional electron density calculations.

### Organic-salt intercalate

The intercalation of organic chain molecules into the layered superconductor has been expected to be one of the most effective methods to investigate the relationship between the structural anisotropy and high- $T_c$  superconductivity, because it allows us to freely regulate the distance between the superconducting cuprate blocks by controlling the carbon number in the organic intercalant. For this reason, many attempts have been made to intercalate the organic molecule into a

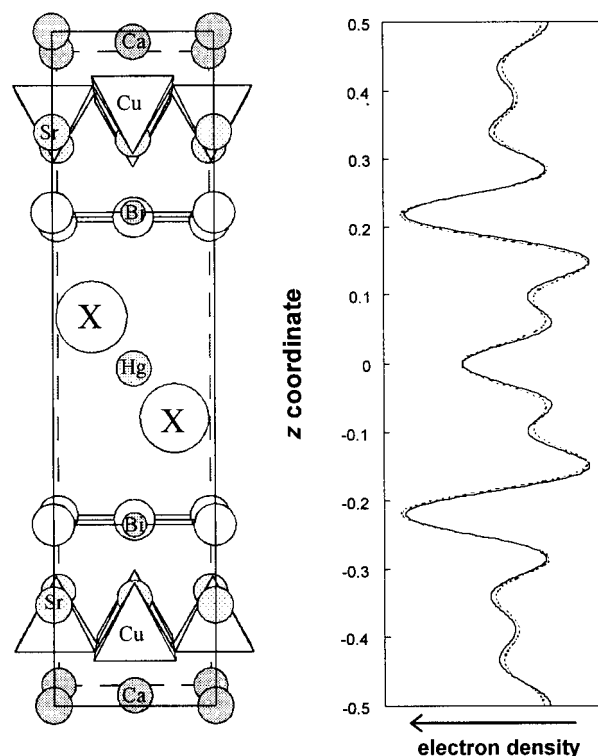
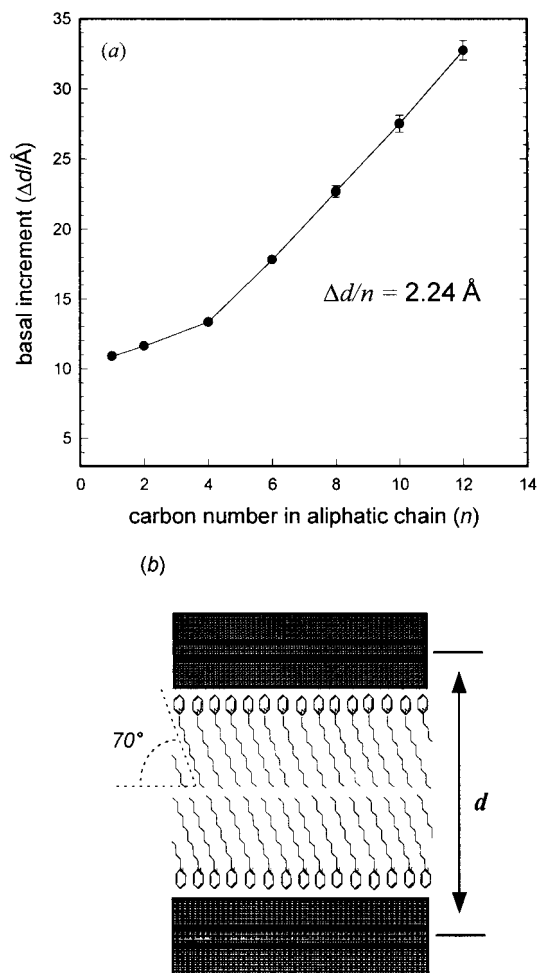


Fig. 2 One-dimensional electron density mappings along the  $c$ -axis of  $(\text{HgX}_2)_{0.5}\text{Bi}_2\text{Sr}_2\text{CaCu}_2\text{O}_y$ , together with the structural model; (—) experimental, (---) calculated.

superconducting lattice, on the basis of the HSAB concept. But, every trial was found only to fail, which might be due to a severe geometric hindrance of the bulky organic molecule. In this respect, we have adopted a new synthetic strategy using interlayer complexation reaction. Taking into account the coordinately unsaturated state of mercury in  $\text{HgX}_2$ -intercalates,<sup>5</sup> it is reasonable to expect that the intercalated mercuric halide species could be further ligated by organic/inorganic ligands in the interlayer space of Bi-based cuprates. Based on this synthetic strategy, we were successful in intercalating organic salts into Bi-based compounds. The formation of single phase stage-1 intercalates was confirmed not only by powder XRD analyses but also by a cross-sectional view of the high-resolution electron microscope (HREM) images. The XRD analyses for the organic-salt-intercalate  $(\text{Py-C}_n\text{H}_{2n+1})_2\text{HgI}_4\text{-Bi}_2\text{Sr}_2\text{Ca}_{m-1}\text{Cu}_m\text{O}_y$  indicate that the basal increment ranges from 10.8–31.6 Å depending on the length of the alkyl chain. The basal spacing of organic-salt-intercalate is plotted in Fig. 3 as a function of carbon number in the organic chain, where the basal increment ( $\Delta d$ ) is linearly proportional to the number of carbon atoms ( $n$ ) in each alkyl chain over the range  $n = 4 - 12$ . From the slope of  $\Delta d/n$  ( $= 2.42$  Å), it is suggested that the bilayered alkyl chains are stabilized inbetween  $\text{Bi}_2\text{O}_2$  layer with a tilt angle of  $\approx 70^\circ$  respect to the basal plane as illustrated in Fig. 3.

The HREM image of the cross-section of the organic-inorganic hybrid  $[(\text{Py-C}_{12}\text{H}_{25})_2\text{HgI}_4\text{-Bi2212}]$  obtained by ultramicrotomy is represented in Fig. 4. It appears to feature well-aligned planes with a periodic arrangement of dark lines and bright ones, where the discrete bright lines represent the intercalated organic bilayers. The basal spacing estimated by the present HREM image ( $d \approx 48$  Å) is consistent with that from XRD analysis.

In relation to the intercalation mechanism of organic intercalates, the intracrystalline structures of the intercalated Hg-I species have been investigated by EXAFS analysis on the Hg  $L_{III}$ -edge for the  $\text{HgI}_2$ -intercalate and the organic-salt one. The  $k^3$  weighted Fourier transforms (FT's) of Hg  $L_{III}$ -



**Fig. 3** (a) The relation between the basal spacing and the alkyl chain length in organic-inorganic nano-hybrids  $(\text{Py-C}_n\text{H}_{2n+1})_2\text{HgI}_4\text{-Bi2212}$ . (b) Schematic illustration of most probable structure of Bi2212 intercalated with  $n$ -decylpyridinium derivatives. It is suggested that complex anion  $\text{HgI}_4^{2-}$  is sandwiched in between the  $n$ -alkylpyridinium cation but omitted here for simplicity.

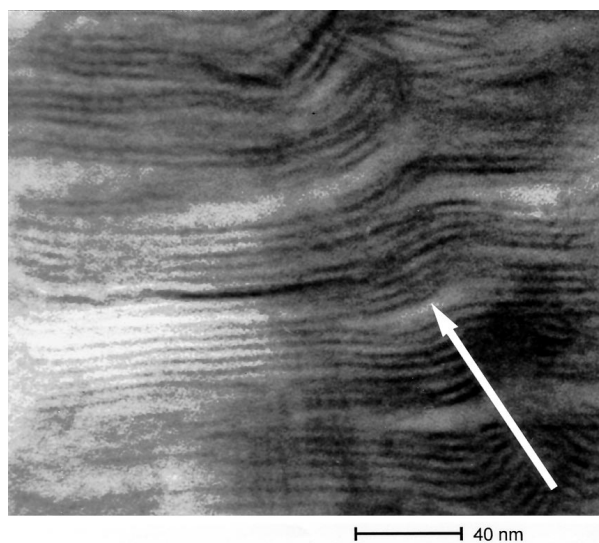


**Fig. 4** A cross-sectional HREM image of  $(\text{Py-C}_{12}\text{H}_{25})_2\text{HgI}_4\text{-Bi2212}$ . The superconducting cuprate layers of 15.4 Å thick are bent by the mechanical strain upon thin-sectioning, where the arrow indicates the cutting direction.

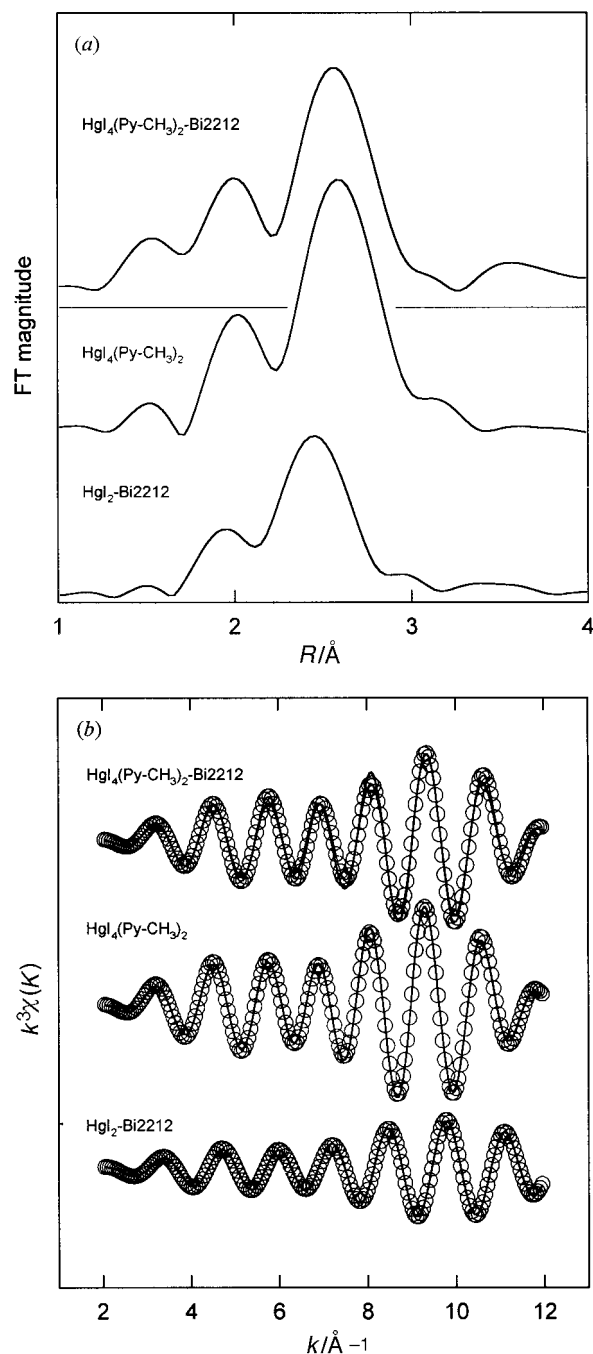


**Fig. 5** (a) Fourier transformation of  $k^3$  weighted Hg  $L_{III}$ -edge EXAFS spectra and (b) their inverse Fourier transforms for  $\text{HgI}_2\text{-Bi2212}$ ,  $(\text{Py-CH}_3)_2\text{HgI}_4\text{-Bi2212}$  and  $(\text{Py-CH}_3)_2\text{HgI}_4$ . The solid line and open circle represent the experimental and calculated data, respectively.

edge EXAFS spectra and their Fourier filtered spectra are shown in Fig. 5(a) and 5(b). From the results of EXAFS curve fitting, the coordination number of Hg was found to increase from two in the  $\text{HgI}_2$ -intercalate<sup>5</sup> to four in the organic-salt one, which is consistent with the reference compound  $(\text{Py-C}_n\text{H}_{2n+1})_2\text{HgI}_4$ .<sup>7</sup> The above result clarifies that the intercalation of organic molecules occurs through the interlayer complexation between intracrystalline  $\text{HgI}_2$  and  $n$ -alkylpyridinium iodide, resulting in the formation of bis( $n$ -alkylpyridinium)tetraiodomercurate,  $(\text{Py-C}_n\text{H}_{2n+1})_2\text{HgI}_4$ . For this reason, the major driving force of organic-salt-intercalation is assigned as a negative enthalpy change during the formation of the tetraiodomercurate complex anion ( $\text{HgI}_4^{2-}$ );  $\text{HgI}_2 + 2\text{I}^- \rightarrow \text{HgI}_4^{2-}$ ,  $\Delta H = -95.8 \text{ kJ mol}^{-1}$ .<sup>26</sup>

According to the dc magnetic susceptibilities for pure Bi2212 and its organic-salt-intercalates, all the organic-salt intercalates are found to exhibit high- $T_c$  superconductivity with the onset  $T_c$  of 80–81 K, which is higher than those for the iodine-intercalate ( $T_c=63$  K,  $\Delta d=3.6$  Å) and for the HgI<sub>2</sub> one ( $T_c=68$  K,  $\Delta d=7.2$  Å), even slightly higher than that for pure Bi2212 ( $T_c=78$  K). Considering the large separation between the superconducting blocks and the small coherence length along the  $c$ -axis in the pure compounds,<sup>27</sup> the high- $T_c$  superconductor interstratified with organic layers can be regarded as a two-dimensional cuprate superconductor with negligible interlayer electronic coupling. Although similar Josephson (S–I–S) coupled multilayers could be fabricated by the sequential deposition of alternate layers of superconducting layers and non-superconducting ones,<sup>28,29</sup> the present organic–inorganic nano-hybrids are believed to be the most suitable model compounds for studying the two-dimensional high- $T_c$  superconductivity, due to completely insulating nature of hydrocarbon molecules in the intercalant layer.<sup>30,31</sup> Moreover, their facility to modify the interlayer distance of superconducting layers allows us to examine systematically the relationship between interlayer distance and the physical properties of layered superconductors.

#### Application of intercalation to the nano-engineering of high- $T_c$ superconductors

From the viewpoint of application, the intercalation of  $n$ -alkylchain derivatives can provide a new way of engineering high- $T_c$  cuprates, since it is possible to obtain ultra-fine superconducting particles by exfoliating them into individual sheets. That is, a remarkable lattice expansion upon intercalation leads to a minimization of chemical binding between superconducting blocks, and therefore the superconducting blocks can be separated from each other by applying an appropriate physico-chemical treatment, as illustrated in Fig. 6. In fact, we were successful in preparing the superconducting colloid suspension by the exfoliation of organic-salt-intercalates. At first, an amorphous superconducting film could be realized by dip-coating the colloid suspension with the Ag substrate and the superconducting Bi2212 thin-film was obtained by heating this film at 800 °C for 6 h. As shown in Fig. 7, the sharp (00 $l$ ) XRD peaks are clearly detected for the heat-treated film, indicating that the single phase Bi2212 grains are well aligned along the  $c$ -axis. The crystal structures of exfoliated particle and as-coated film have also been examined by performing electron diffraction (ED) analyses [Fig. 8(a) and (b)]. While the ED pattern of each exfoliated particle exhibits the characteristic atomic arrangement of [100]<sub>Bi2212</sub> and [010]<sub>Bi2212</sub>, clarifying the retention of the oxide lattice even after exfoliation, the ED pattern of as-coated film represents concentric circles together with some spot patterns, represents concentric circles together with some spot patterns,

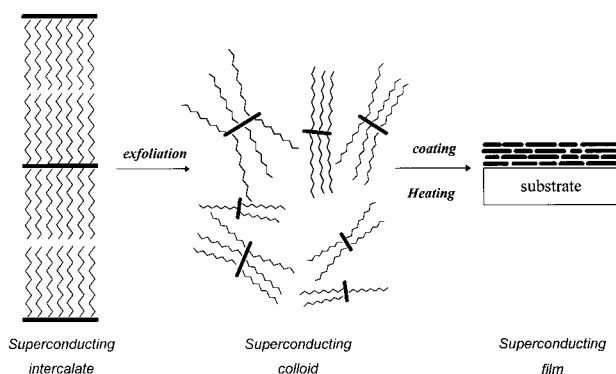


Fig. 6 Schematic diagram for the synthesis of superconducting thin films using intercalation techniques.

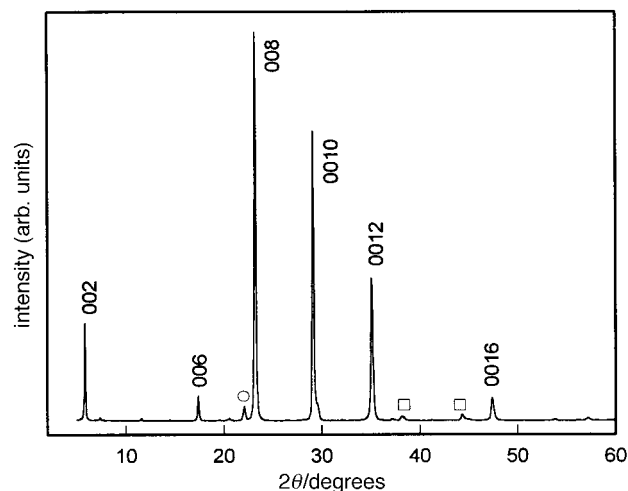


Fig. 7 XRD patterns for superconducting thin film after heat treatment. The XRD reflections originated from other phases are denoted as open squares for Ag substrate and as open circles for impurity Bi2201.

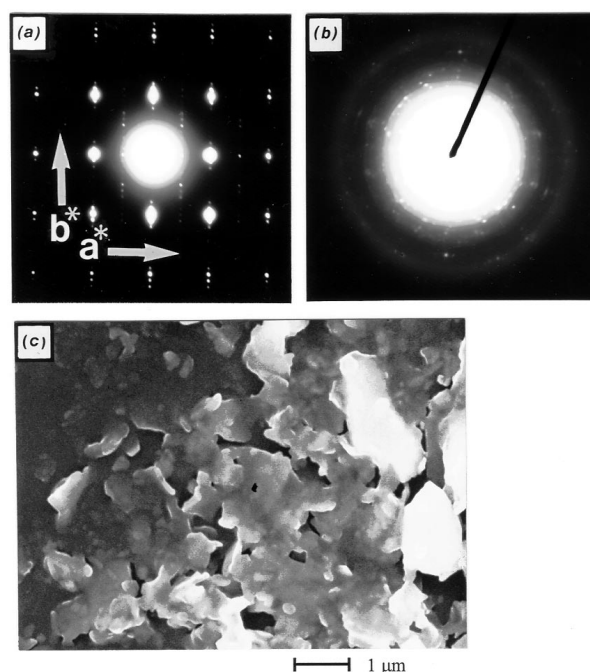


Fig. 8 Electron diffraction patterns for (a) individual particles after exfoliation and (b) as-coated films. (c) Scanning electron micrograph of the substrate surface after dip-coating.

suggestive of face-to-face stacking of the exfoliated cuprate sheets. For the as-coated film, the surface morphology has been investigated by obtaining a scanning electron micrograph (SEM), which reveals that the superconducting layers are stacked parallel to the surface [Fig. 8(c)].

Compared to the conventional methods for fabricating superconducting thin-films such as RF-sputtering, chemical vapor deposition, *etc.*, the present method *via* an intercalation complex is believed to be quite simple and economic. In addition to thin-films, this method can also be applied to the preparation of superconducting tapes and wires, by performing continuous dip-coating and heating processes. Moreover, since Bi-based cuprate superconductors have a high critical field ( $H_{c2}$ ), enough for high-field application, the present intercalation/exfoliation route would be quite useful in fabricating advanced high-magnetic-field equipment.

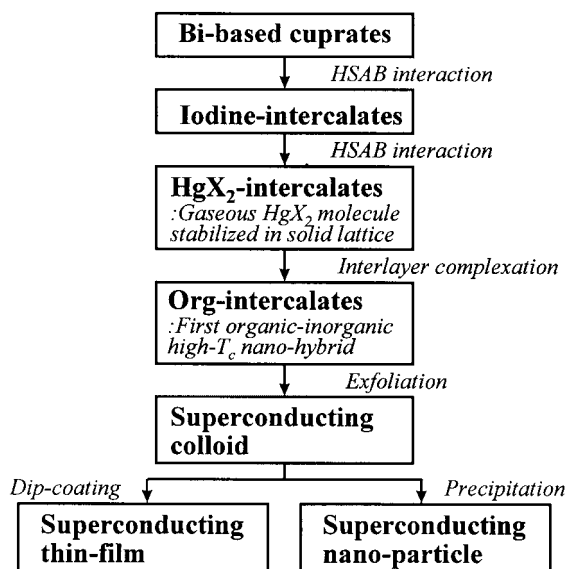


Fig. 9 Flow chart of the synthetic strategy for developing new inorganic-inorganic and organic-inorganic nano-hybrids.

## Conclusion

In this paper, a new type of inorganic-inorganic and organic-inorganic high- $T_c$  superconducting nano-hybrids are presented for the first time by adopting unique synthetic strategies of HSAB intercalation and interlayer complexation concepts, as plotted in Fig. 9. As expected, the systematic XANES/EXAFS analyses clarify that the intercalation of metal halides is surely a kind of Lewis acid-base reaction and that the intercalation of organic molecules is achieved through interlayer complexation. For the organic-salt intercalates, the relationship between basal increment and superconducting property has been systematically investigated, which indicates that the superconductivity of high- $T_c$  cuprates is governed by the intrinsic property of the  $\text{CuO}_2$  plane. Since the present organic-salt intercalates are also weakly coupled Josephson (S-I-S) multilayers with a controllable thickness of insulating layer, they are expected to be most suitable for studying two dimensional superconducting properties. Moreover, these compounds have a potential applicability for the nano-engineering of high- $T_c$  superconductors such as nano-particles and ultra-thin-films. From the viewpoint of material design, the present novel method of stepwise intercalation provides a new synthetic route to a variety of nano-hybrids.

This work was supported in part by the Ministry of Education (BSRI-97-3413) and by the Korean Science and Engineering Foundation through the Center for Molecular Catalysis.

## References

- 1 M. S. Dresselhaus (Editor), *Intercalation in Layered Materials*, Plenum Press, New York, 1986.
- 2 J. M. Wheatly, T. C. Hsu and P. W. Anderson, *Nature*, 1988, **333**, 121.
- 3 X.-D. Xiang, S. McKernan, W. A. Vareka, A. Zettl, J. L. Corkill, T. W. Barbee III and M. L. Cohen, *Nature*, 1990, **348**, 145.
- 4 J. H. Choy, N. G. Park, S. J. Hwang, D. H. Kim and N. H. Hur, *J. Am. Chem. Soc.*, 1994, **116**, 11564.
- 5 J. H. Choy, S. J. Hwang and N. G. Park, *J. Am. Chem. Soc.*, 1997, **119**, 1624.
- 6 J. H. Choy, N. G. Park, Y. I. Kim, S. H. Hwang, J. S. Lee and H. I. Yoo, *J. Phys. Chem.*, 1995, **99**, 7845.
- 7 J. H. Choy, S. J. Kwon and G. S. Park, *Science*, 1998, **280**, 1589.
- 8 J. H. Choy, N. G. Park, S. J. Hwang and Z.-G. Khim, *J. Phys. Chem.*, 1996, **100**, 3783.
- 9 J. H. Choy, S. J. Hwang and D.-K. Kim, *Phys. Rev. B*, 1997, **55**, 5674.
- 10 J. H. Choy, D. K. Kim, S. G. Kang, D. H. Kim and S. J. Hwang, in *Superconducting Materials*, IITT-International, eds. J. Etourneau, J. B. Torrance and H. Yamauch, Paris, 1993, p. 335.
- 11 W. A. Groen, D. M. de Leeuw and G. M. Stollman, *Solid State Commun.*, 1989, **72**, 697.
- 12 A. Maeda, M. Hase, I. Tsukada, K. Noda, S. Takebayashi and K. Uchinokura, *Phys. Rev. B*, 1990, **41**, 6418.
- 13 J. Tsuchiya, H. Endo, N. Kijima, A. Sumiyama, M. Mizuno and Y. Oguri, *Jpn. J. Appl. Phys. Part 2*, 1989, **28**, L1918.
- 14 M. Di Stasio, K. A. Muller and L. Pietronero, *Phys. Rev. Lett.*, 1990, **64**, 2827.
- 15 R. Liu, M. V. Klein, P. D. Han and D. A. Payne, *Phys. Rev. B*, 1992, **45**, 7392.
- 16 K. Yvon and M. Francois, *Z. Phys. B*, 1989, **76**, 413.
- 17 P. V. Huang and A. L. Verma, *Phys. Rev. B*, 1993, **48**, 9869.
- 18 J. H. Choy, S. J. Hwang and W. Lee, *J. Solid State Chem.*, in the press.
- 19 T. Huang, M. Itoh, J. Yu, Y. Inaguma and T. Nakamura, *Phys. Rev. B*, 1994, **49**, 9885 and refs. listed in Table 2.
- 20 X.-D. Xiang, W. A. Vareka, A. Zettl, J. L. Corkill, T. W. Barbee III, M. L. Cohen, N. Kijim and R. Gronsky, *Science*, 1991, **254**, 1487 and refs. listed in Table 2.
- 21 J. E. Huheey, E. A. Keiter and R. L. Keiter, *Inorganic Chemistry*, Harper Collins College Publishers, New York, 1993.
- 22 J. B. Boyce, T. M. Hayes, W. Stutius and J. C. Mikkelsen, Jr., *Phys. Rev. Lett.*, 1977, **38**, 1362.
- 23 M. J. Rice and W. L. Roth, *J. Solid State Chem.*, 1972, **4**, 294.
- 24 S. Geller, *Science*, 1967, **157**, 310.
- 25 A. F. Wells, *Structural Inorganic Chemistry*, Clarendon Press, Oxford, 1984.
- 26 R. Arnek and D. Poceva, *Acta Chem. Scand., Ser. A*, 1976, **30**, 59.
- 27 R. Kleiner and P. Müller, *Phys. Rev. B*, 1994, **49**, 1327.
- 28 Q. Li, Ø. Fischer, O. Brunner, L. Antognazza, A. D. Kent and M. G. Karkut, *Phys. Rev. Lett.*, 1990, **64**, 3086.
- 29 J. M. Triscone, X. X. Xi, X. D. Wu, A. Inam, S. Vadlamannati, W. L. McLean, T. Veukatesan, R. Ramesh, D. M. Hwang, J. A. Martinez and L. Nazar, *Phys. Rev. Lett.*, 1990, **64**, 804.
- 30 D. R. Nelson, *Nature*, 1995, **375**, 356.
- 31 E. Zeldov, D. Majer, M. Konczykowski, V. B. Geshkenbein, V. M. Vinokur and H. Shtrikman, *Nature*, 1995, **375**, 373.

Paper 8/05869E